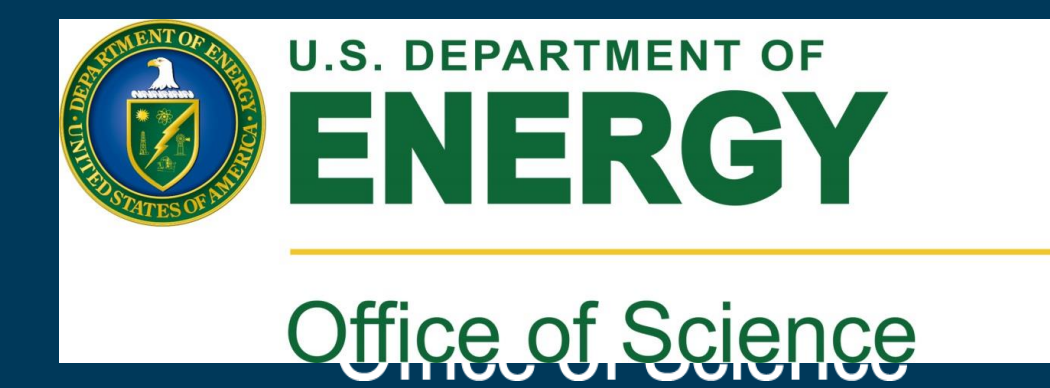


# Strain Engineering of 2D Valleytronic Materials from *Ab-Initio* Theory

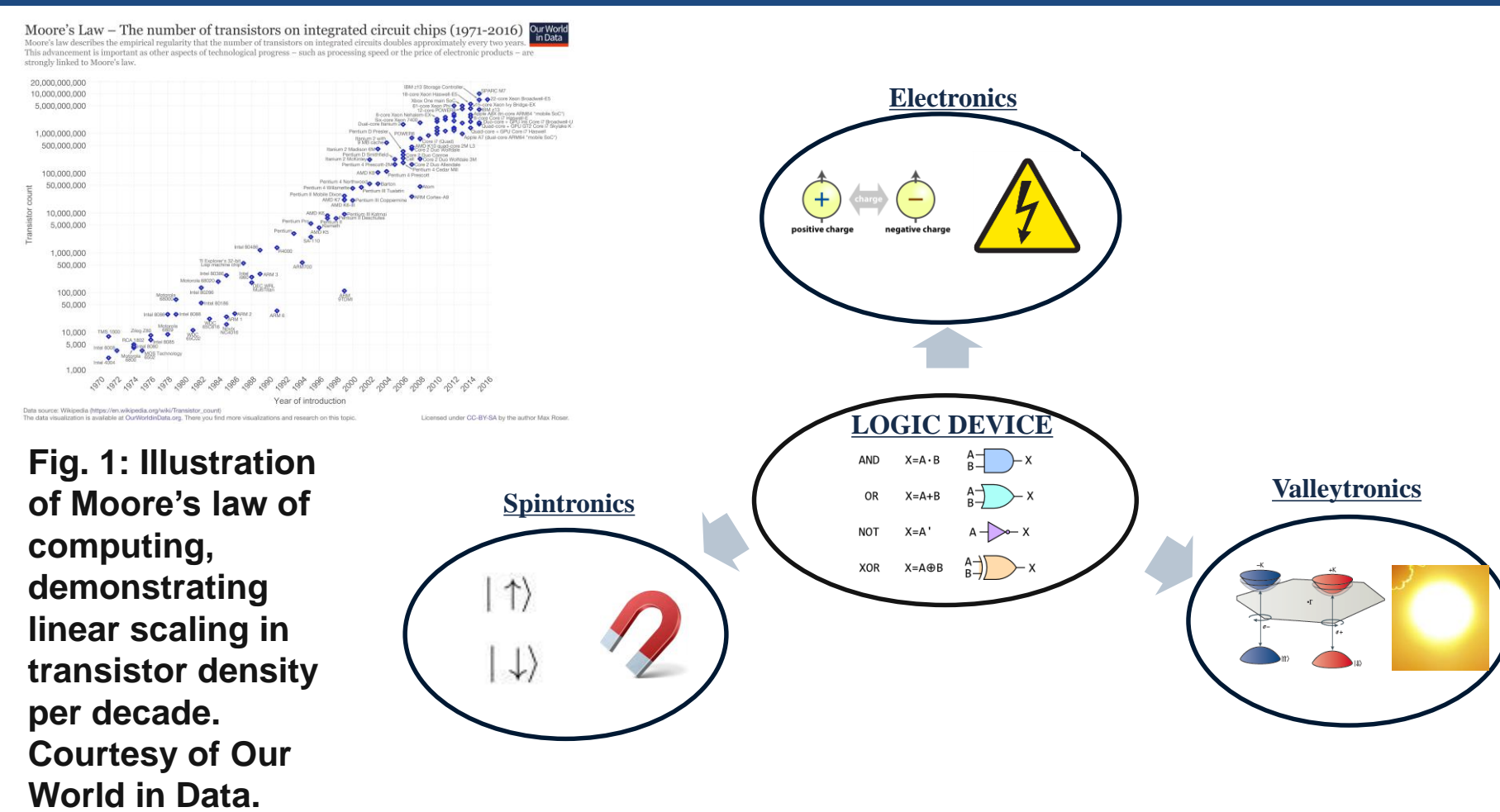


Nima Leclerc<sup>1</sup>, Jonah Haber<sup>2</sup>, Jefferey B. Neaton<sup>2</sup>  
<sup>1</sup>Cornell University, <sup>2</sup>Lawrence Berkeley National Laboratory

## Abstract

Recent developments in valleytronics demonstrate that exceptional 2D transition metal dichalcogenides (TMDs) can selectively switch between valley logic states, '0' and '1' since 2D TMDs possess degenerate energy levels at the K and K' valleys in reciprocal space. This unique valley physics can give rise to more energy efficiency transistors. This is because the states can be controlled by photoexcitation rather than an external gate voltage. In spite of this energy efficiency feature, phonon-assisted intravalley scattering that occur during excitations degrades the coherence times of these states although their spatially separation maintains state protection. Moreover, an understanding of the strain effects on phonon-assisted intravalley scattering has yet quantified. Considering this we investigate the effects of strain on the carrier lifetimes, vibrational modes, and fundamental electronic properties of MoS<sub>2</sub> using first principles Density Functional Theory (DFT) calculations. In particular, we apply biaxial tensile strain to monolayer MoS<sub>2</sub> to suppress these phonon-assisted scattering pathways to effectively localize excitations at K and K' valleys.

## Valleytronics: Pushing Beyond Moore's Law



**Valley (Def.):** Region in reciprocal space in the vicinity of the conduction/valence band extrema

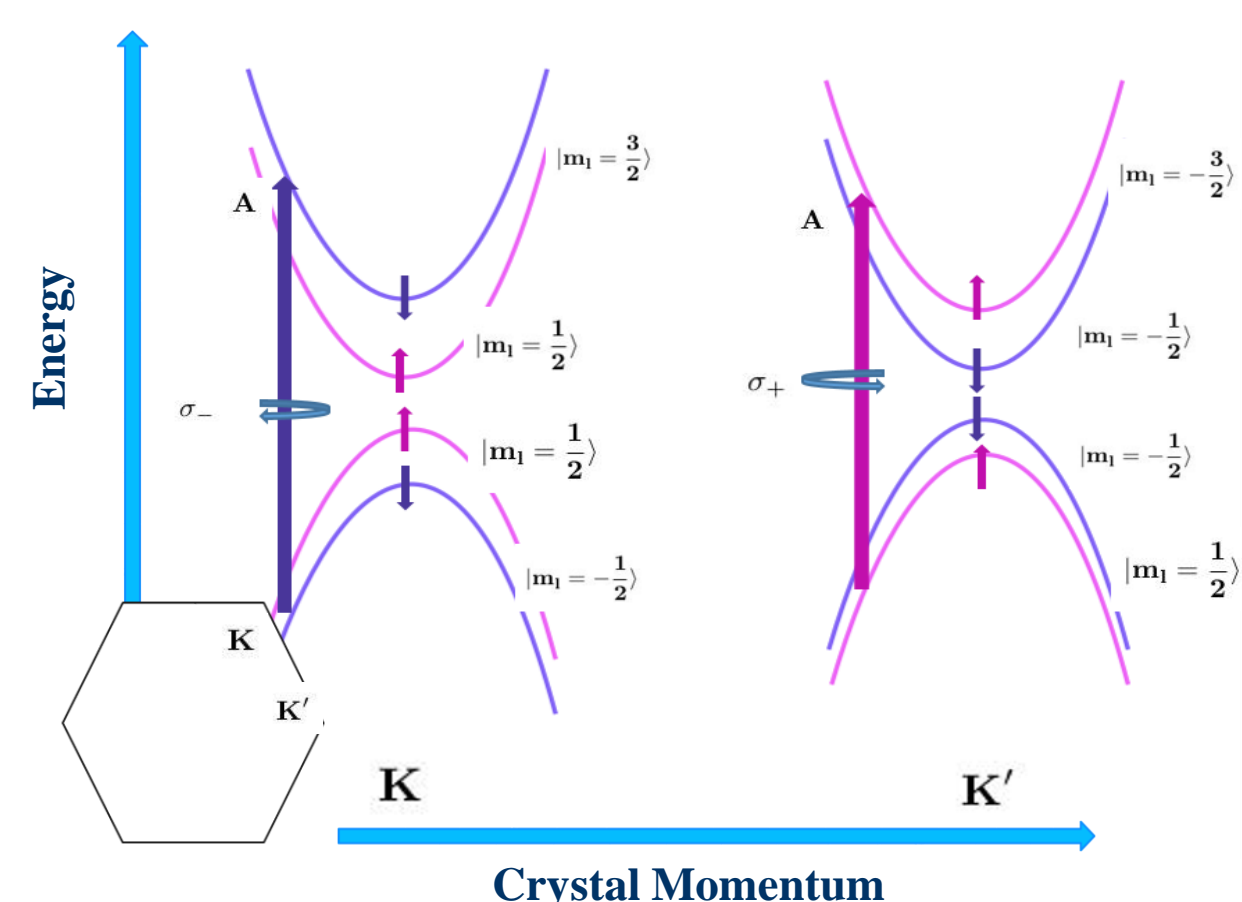


Fig. 2: Schematic of spin-split degenerate energy level at K and K' valleys in 2D MoS<sub>2</sub>.  $\sigma_{\pm}$  denotes excitations via right/left circularly polarized photons, A denotes first order exciton recombination energy. Purple and pink bands demonstrate prevalent spin-orbit interactions in MoS<sub>2</sub>. 2D MoS<sub>2</sub> hexagonal Brillouin zone (BZ) depicted in lower-left hand corner.

## Novel Approach: strain engineering 2D Valleytronics to suppress Phonon Scattering

### Electronic Structure w/ Strain

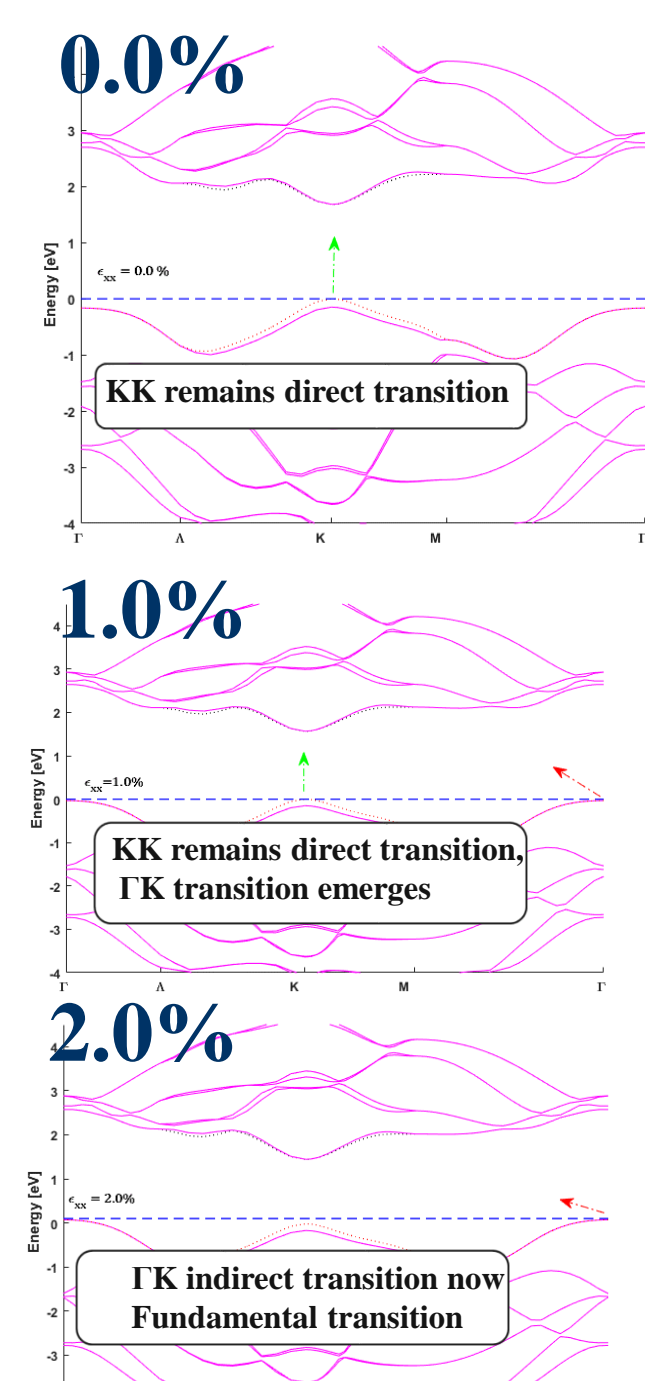


Fig. 3: Computed band structure in 2D MoS<sub>2</sub> with strain, using GGA functionals with spin-orbit. Dashed blue line depicts position of Fermi level.

### (1) Density Functional Theory (DFT) Ground State with Tensile Strain

$$E_{KS}[n] = -\frac{1}{2} \sum_{i,\sigma} \langle \psi_i^\sigma | \nabla^2 | \psi_i^\sigma \rangle + \int d^3r \hat{V}_{ext}(\mathbf{r})n(\mathbf{r}) + E_{II}[n] + E_H[n] + E_{GGA}[n]$$

### (2) Obtain Electronic Structure

$$(H_{KS}(\mathbf{k}) - \epsilon_n(\mathbf{k}))\phi_{n,\mathbf{k}}^{KS} = 0$$

Approach employed DFT to obtain ground-state eigenvalues and wavefunctions defining the electronic structure (ES). Tracking ES with induced strain plays a chief role in understanding crossovers in probable electronic transition associated with relevant valley states and selection rules. Band calculations revealed that direct (KK) to indirect (K $\Gamma$ ) energetic crossover emerges at 2.0% tensile strain. pDOS calculation reveals that selection rules are robust to this range of tensile strain. Direct KK transition is necessary in devices for state protection.

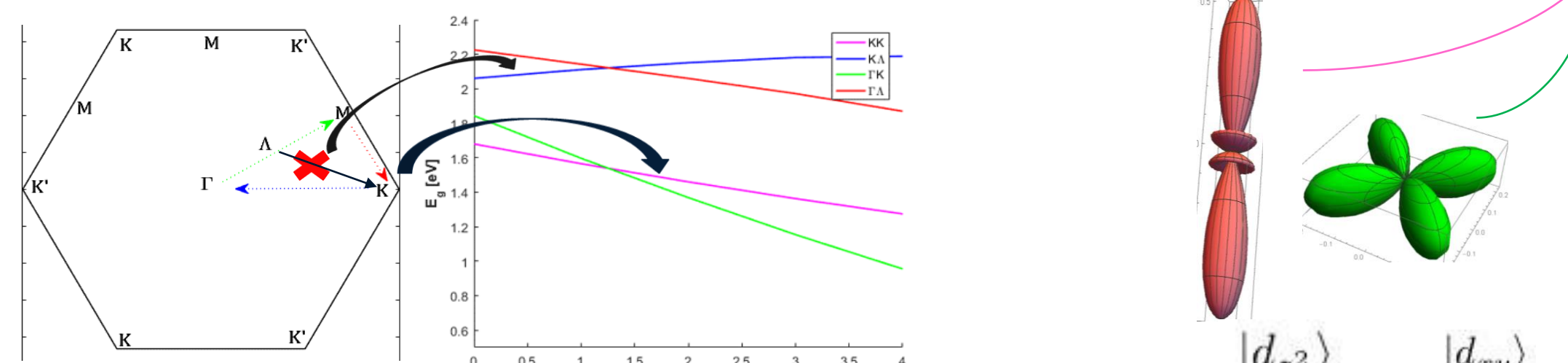


Fig. 4: Schematic of 1<sup>st</sup> BZ of 2D MoS<sub>2</sub> (left), with dotted arrows depicting reduced  $k$ -path taken & parasitic KA. Plot of DFT-computed KK, KA, FK, &  $\Gamma$ A energy (in eV) transitions in 2D MoS<sub>2</sub> with biaxial strain. Indicates parasitic KA transition being suppressed and KK preferred direct gap closing with increased tensile strain.

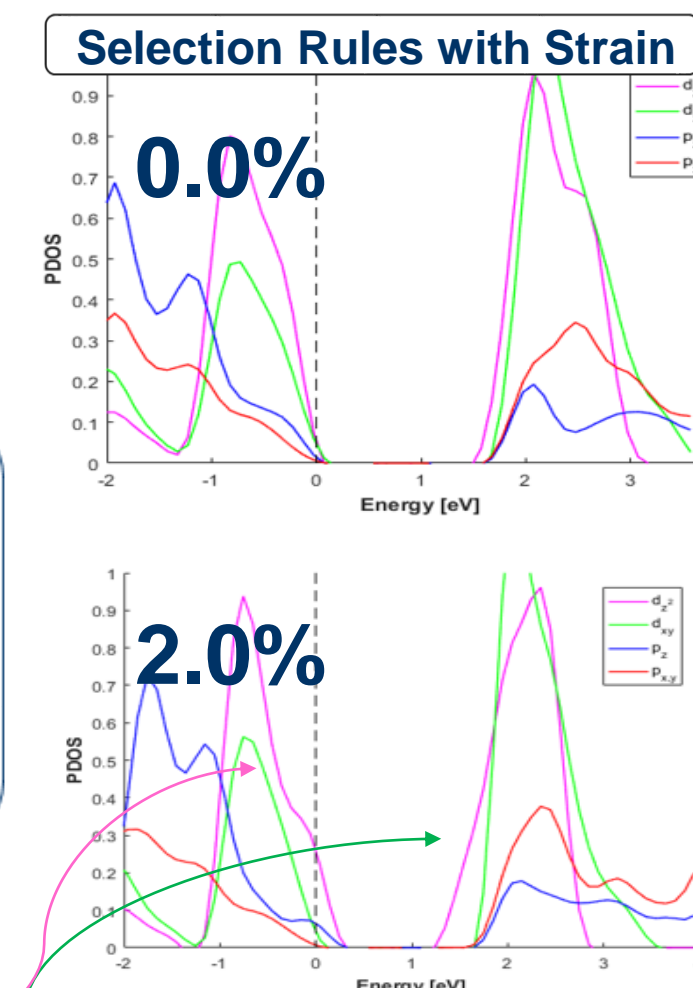
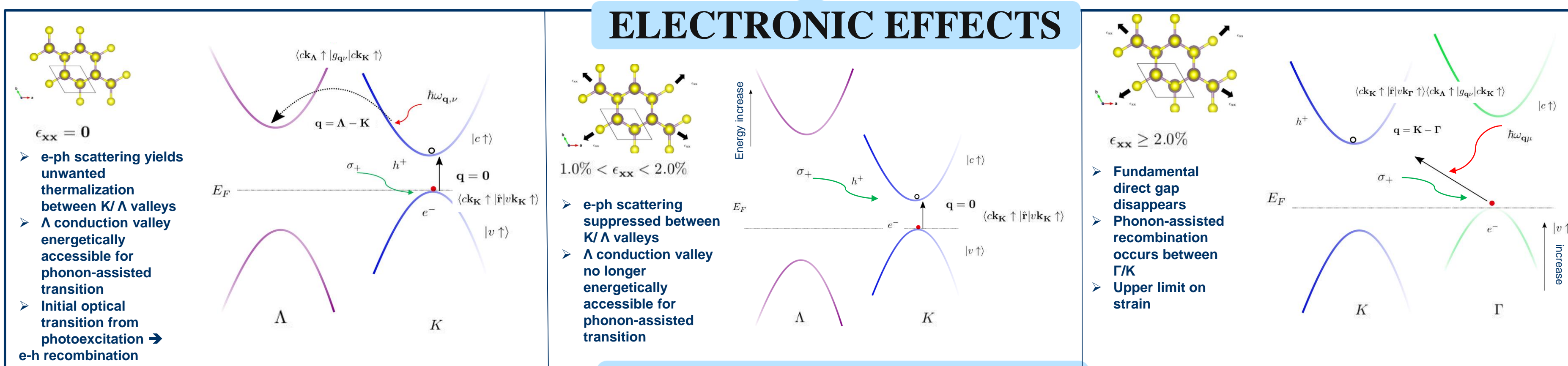


Fig. 5: Computed Projected Density of States in 2D MoS<sub>2</sub> for equilibrium and 2.0% strained systems. Horizontal axis in eV. Position of the Fermi level represented by vertical dashed line centered at 0 eV. Demonstrates that predominant orbital character near the Fermi level remains  $d_{xy}$  &  $d_{z^2}$  with tensile strain, hence preserves optical selection rules.

## ELECTRONIC EFFECTS



## VIBRATIONAL EFFECTS

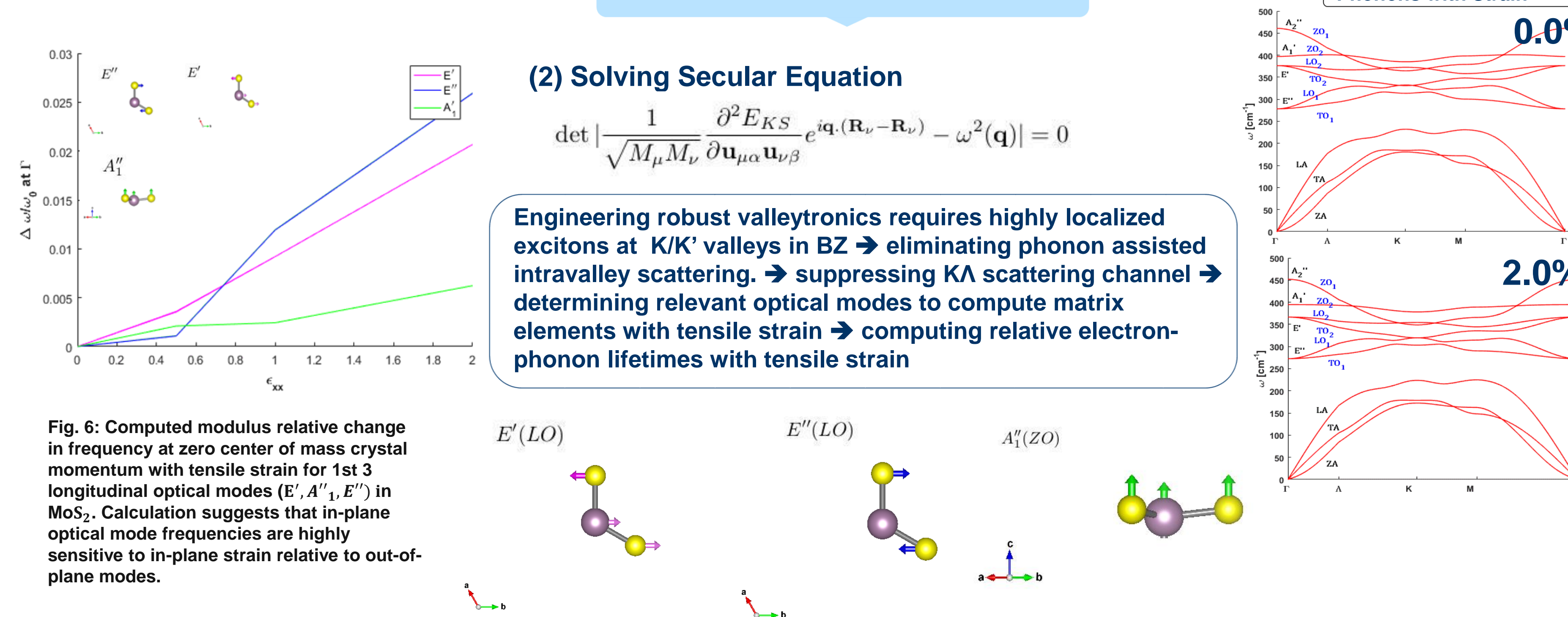


Fig. 6: Computed modulus relative change in frequency at zero center of mass crystal momentum with tensile strain for 1<sup>st</sup> 3 longitudinal optical modes ( $E'$ ,  $A''$ ,  $E''$ ) in MoS<sub>2</sub>. Calculation suggests that in-plane optical mode frequencies are highly sensitive to in-plane strain relative to out-of-plane modes.

### (2) Solving Secular Equation

$$\det \left[ \frac{1}{\sqrt{M_\mu M_\nu}} \frac{\partial^2 E_{KS}}{\partial u_{\mu\alpha} \partial u_{\nu\beta}} e^{i\mathbf{q} \cdot (\mathbf{R}_\nu - \mathbf{R}_\mu)} - \omega^2(\mathbf{q}) \right] = 0$$

Engineering robust valleytronics requires highly localized excitons at K/K' valleys in BZ  $\rightarrow$  eliminating phonon assisted intravalley scattering.  $\rightarrow$  suppressing KA scattering channel  $\rightarrow$  determining relevant optical modes to compute matrix elements with tensile strain  $\rightarrow$  computing relative electron-phonon lifetimes with tensile strain

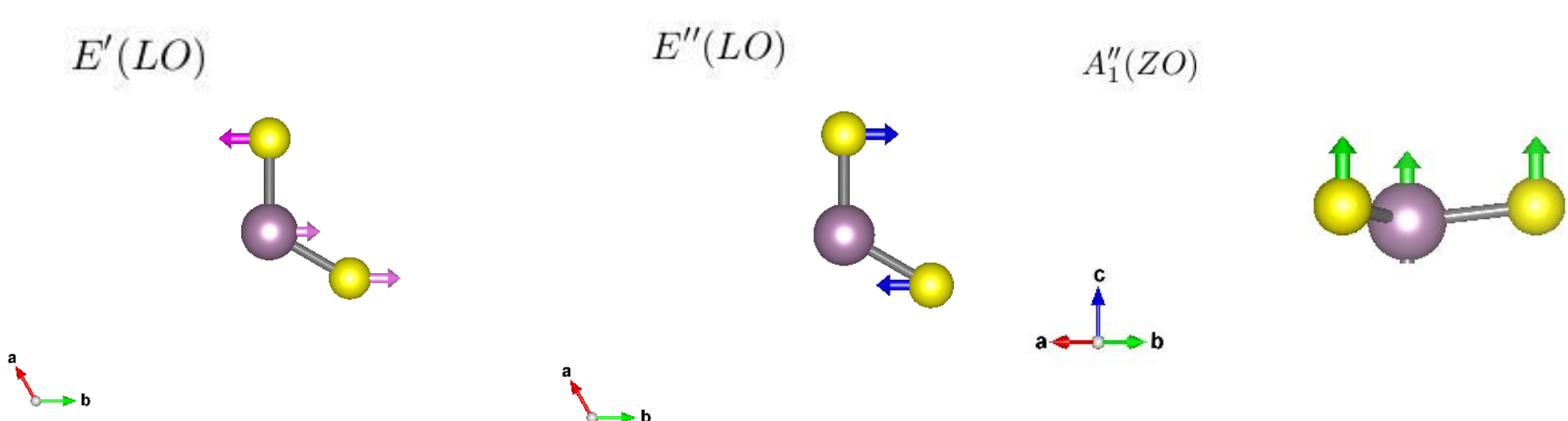


Fig. 7:  $E'$ ,  $A''$ ,  $E''$  optical modes in MoS<sub>2</sub> (purple spheres are Mo atoms and yellow spheres are S atoms) (left). Computed phonon dispersions in 2D MoS<sub>2</sub>, depicting all 9 eigenfrequencies [ $\text{cm}^{-1}$ ] along  $\Gamma$ -A-K-M- $\Gamma$   $q$ -path. Calculation reveal overall decrease in phonon frequency with tensile strain (above right).

## Magic of Quantum Confinement

### Breaking Inversion Symmetry in MoS<sub>2</sub> to Control Electrons

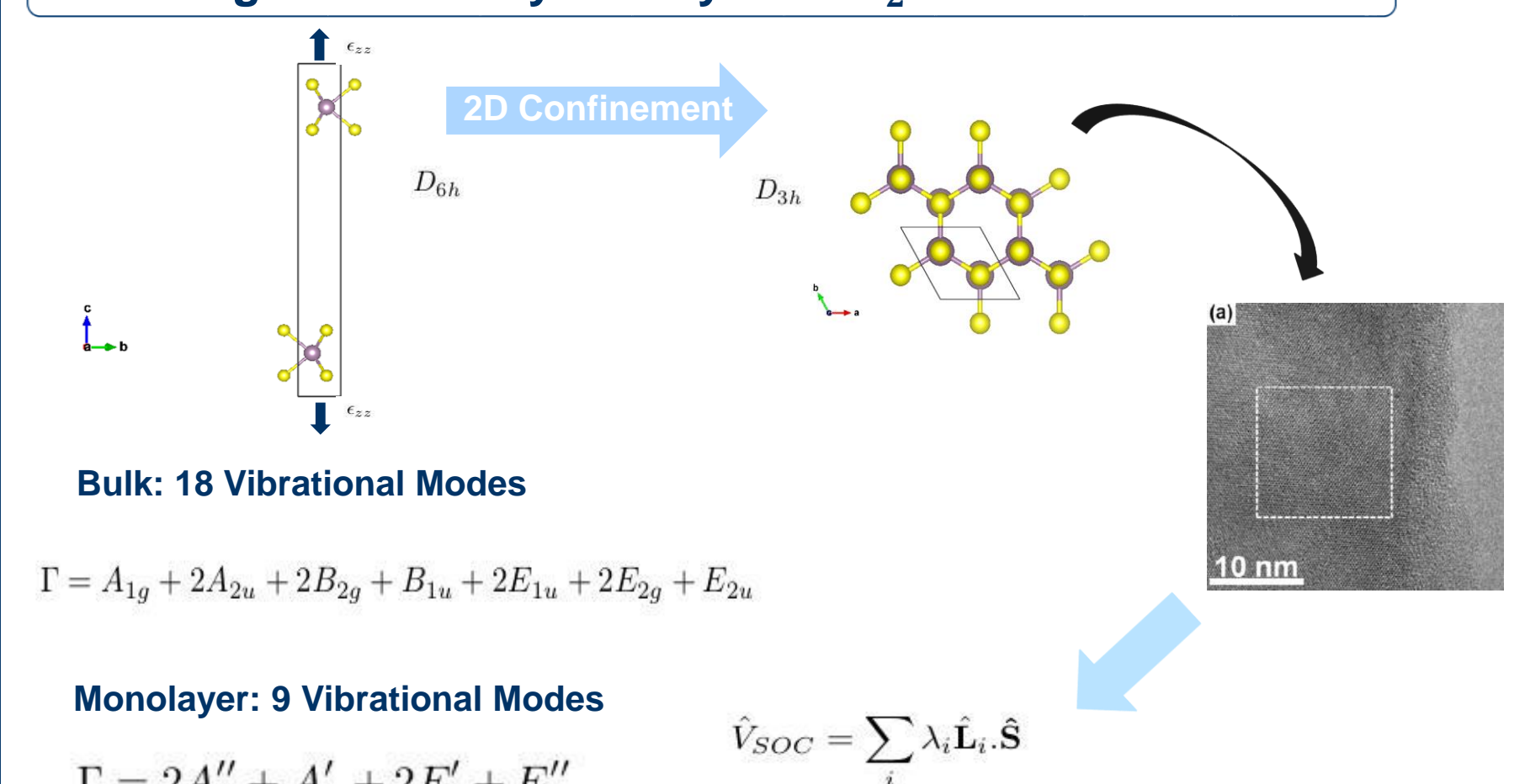


Fig. 8: Bulk bilayer MoS<sub>2</sub> with applied strain along  $c$  axis, depicting layers interacting via Van der Waal Interactions [Mo atoms in purple, S atoms in yellow] (upper left), monolayer MoS<sub>2</sub> structure illustrating break in inversion symmetry (upper middle), cross sectional Transmission Electron Microscope image of monolayer MoS<sub>2</sub> courtesy of Lin *et al.* (upper right). Confinement gives rise to stronger spin-orbit interactions from Mo  $d$  orbitals and reduction in the number of relevant phonon modes.

### Changing Electronic and Optoelectronic Properties

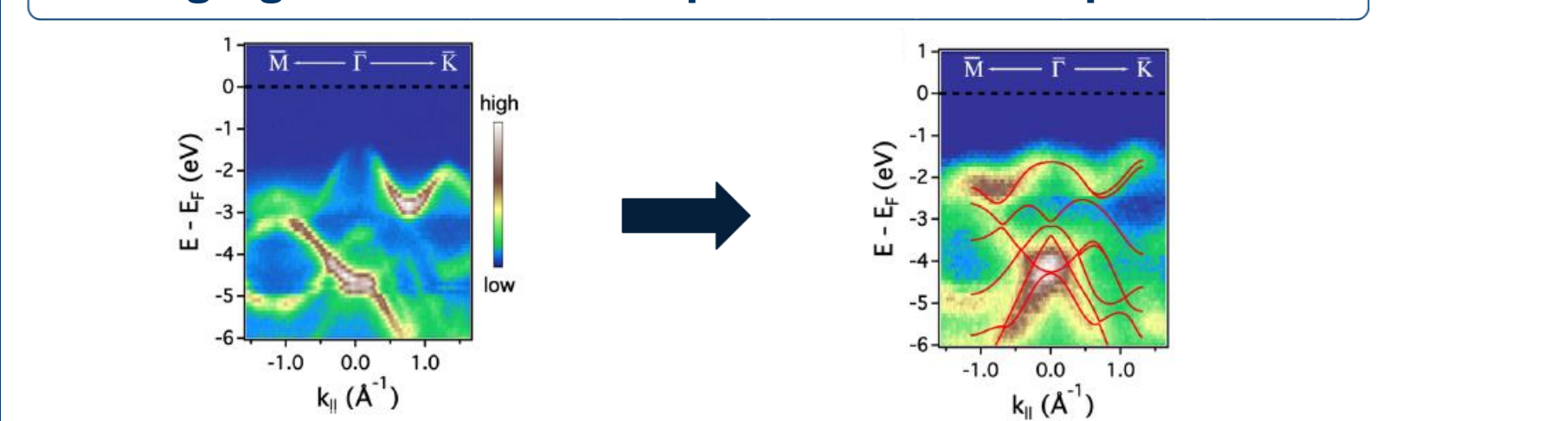


Fig. 9: Angle Resolved Photoemission Spectroscopy band structure measurements of bulk (left) and monolayer (right) MoS<sub>2</sub>, depicting indirect to direct band gap transition at K point in BZ. Experimental measurements courtesy of Osgood *et al.*

## Next Step- Strain Engineered Scattering

(1) Use Fermi's Golden rule for determination of scattering rates w/Strain

$$\frac{1}{\tau_{nk}} = \frac{2\pi}{\hbar} \sum_{m\nu} \int \frac{d\mathbf{q}}{\Omega_{BZ}} |g_{nm}(\mathbf{k}, \mathbf{q})|^2 \times [(1 - f_{m\mathbf{k}+\mathbf{q}} + n_{q\nu})\delta(\epsilon_{nk} - \hbar\omega_{q\nu} - \epsilon_{m\mathbf{k}+\mathbf{q}}) + (f_{m\mathbf{k}+\mathbf{q}} + n_{q\nu})\delta(\epsilon_{nk} + \hbar\omega_{q\nu} - \epsilon_{m\mathbf{k}+\mathbf{q}})]$$

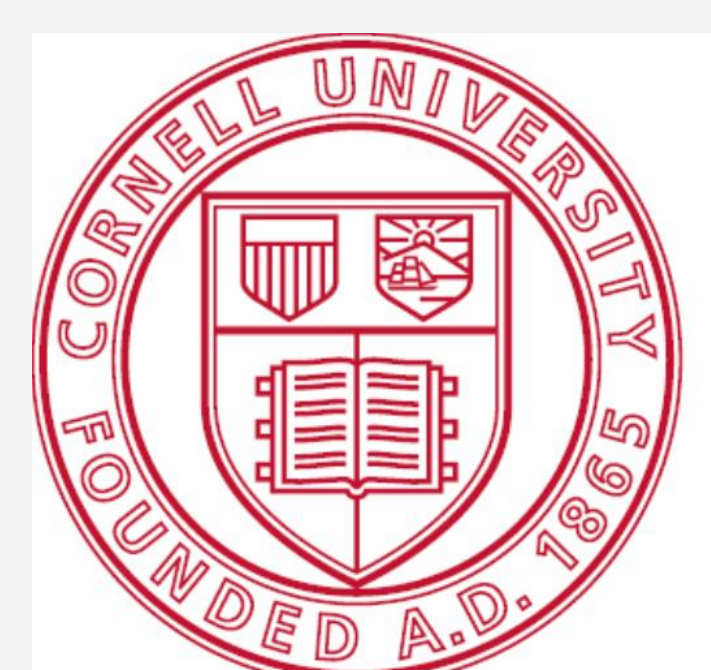
Expression determines scattering of an electron at band index  $n$  and point  $\mathbf{k}$  in the Brillouin zone by distance  $\mathbf{q}$  in momentum space to a band of index  $m$ , via a phonon of index  $\nu$ .

Used to probe transport properties with strain

(2) Compute optical properties with tensile strain, use Bethe-Salpeter Equation and Many-Body Green's Function approach

## Acknowledgments

This work was supported in part by the U.S. Department of Energy, Office of Science, Office of Workforce and Development for Teachers and Scientists (WDTs) under the Science Undergraduate Laboratory Internship (SULI) program. This work is would not be possible without the Theory of Nanostructured Materials Facility at the Molecular Foundry and the National Research Scientific Computing Center for supporting this work. Acknowledgments to Jonah Haber and Jefferey B. Neaton for excellent mentorship in completing this work.



Cornell University



MOLECULAR FOUNDRY

NERSC

THE KAVLI FOUNDATION

